

Near-threshold K^-d scattering and properties of kaonic deuterium

N.V. Shevchenko

Nuclear Physics Institute, 25068 Řež, Czech Republic

Abstract

We calculated the $1s$ level shifts and widths of kaonic deuterium, corresponding to accurate results on near-threshold antikaon - deuteron scattering. The Lippmann-Schwinger eigenvalue equation with a strong $K^- - d$ and Coulomb potentials was solved. The two-body $K^- - d$ potentials reproduce the near-threshold elastic amplitudes of K^-d scattering obtained from the three-body Alt-Grassberger-Sandhas equations with the coupled channels using four versions of the $\bar{K}N - \pi\Sigma$ potentials. Both new $\bar{K}N - \pi\Sigma$ potentials reproducing the very recent SIDDHARTA data on kaonic hydrogen and our older potentials reproducing KEK data have one- or two-pole versions of the $\Lambda(1405)$ resonance and reproduce experimental data on K^-p scattering.

Keywords: mesonic atom, antikaon-nucleon interaction, scattering length, few-body equations

1. Introduction

Kaonic atoms as well as scattering of antikaons on nuclei can be used for investigation of antikaon-nucleon interaction. Deuteron is a particularly promising target since dynamics of the few-body K^-d system can be properly described by Faddeev equations. In our previous paper [1] we used the equations for calculations of the K^-d scattering length a_{K^-d} and investigated its dependence on the two-body input. In particular, we were interested in dependence of a_{K^-d} on phenomenological models of the $\bar{K}N$ interaction with one or two poles forming $\Lambda(1405)$ resonance since the question of number of the poles is quite actual (see e.g. [2, 3]).

In spite of the fact that the most of the “chirally based” models of the interaction have two poles, such two-pole structure and energy dependence

are not necessary for reproducing experimental data on K^-p scattering and kaonic hydrogen. It was clearly shown in [1, 4], where all the data were described by energy-independent $\bar{K}N - \pi\Sigma$ potentials having one- or two-pole structure with equally high accuracy. It was also demonstrated that no experimental data prove the two-pole structure of the $\Lambda(1405)$ resonance.

However, the scattering length, in contrast to the $1s$ level shift and width of kaonic deuterium, cannot be measured directly. The task of calculation of the kaonic deuterium characteristics is quite actual in view of SIDDHARTA-2 experiment [5], planning measurements of the atom.

Mixture of strong and Coulomb interactions complicates theoretical investigation of low levels of hadronic atoms using methods of few-body physics. Due to this we calculated the energy of the $1s$ level considering kaonic deuterium as a two-body $K^- - d$ system. For this purpose a strong $K^- - d$ potential, reproducing the K^-d scattering observables obtained in the advanced calculation, was constructed. However, additional three-body calculations were necessary to be done before.

First, the potentials used in the calculations in [1] reproduce the KEK data on the kaonic hydrogen characteristics together with all experimental data on low-energy K^-p scattering. Keeping in mind the very recent data on kaonic hydrogen measured in the SIDDHARTA experiment [6], we constructed the new $\bar{K}N - \pi\Sigma$ potentials, which reproduce the newest experimental data, and repeated the calculations of the K^-d scattering length.

Second, knowledge of the scattering length is not enough for construction of the $K^- - d$ potential, therefore, we additionally calculated the near-threshold K^-d scattering amplitudes for all four models of antikaon-nucleon interaction: used in [1] and the new ones. Effective ranges were calculated as well. Finally, the results of the three-body calculations were used for construction of the strong $K^- - d$ potentials. The $1s$ level shifts and widths of kaonic deuterium were then obtained by solving the Lippmann-Schwinger eigenvalue equation with the constructed strong potentials and directly included Coulomb interaction.

An effective two-body $K^- - d$ potential was used for calculation of level shifts and widths of kaonic deuterium in [7]. The zero-range potential, used in the paper, reproduces a three-body K^-d scattering length only.

The first subsection of the next section is devoted to the new $\bar{K}N - \pi\Sigma$ potentials, while the rest of the two-body input and the three-body formalism used for the calculations of the near-threshold elastic K^-d amplitudes are described in subsection 2.2. The obtained K^-d scattering lengths and three-

body amplitudes are demonstrated and discussed in the last subsection of Section 2. Section 3 contains description of the two-body strong $K^- - d$ potential together with the method of the calculation of the $1s$ level energy of kaonic deuterium. The results are shown and discussed in section 4, the last section concludes the article.

2. Near-threshold $K^- d$ scattering

2.1. $\bar{K}N - \pi\Sigma$ potentials reproducing SIDDHARTA data

All $\bar{K}N - \pi\Sigma$ potentials used in our previous work [1] for the $K^- d$ scattering length calculations reproduce, among other experimental data, the $1s$ level shift ΔE_{1s} and width Γ_{1s} of kaonic hydrogen, measured in KEK [8]:

$$\Delta E_{1s}^{\text{KEK}} = -323 \pm 63 \pm 11 \text{ eV}, \quad \Gamma_{1s}^{\text{KEK}} = 407 \pm 208 \pm 100 \text{ eV}. \quad (1)$$

In what follows the two representative potentials from Ref. [1], having one and two poles forming the $\Lambda(1405)$ resonance, will be denoted by $V_{\bar{K}N-\pi\Sigma}^{1,\text{KEK}}$ and $V_{\bar{K}N-\pi\Sigma}^{2,\text{KEK}}$ respectively. Recently, new data on kaonic hydrogen were obtained by the SIDDHARTA collaboration [6]:

$$\Delta E_{1s}^{\text{SIDD}} = -283 \pm 36 \pm 6 \text{ eV}, \quad \Gamma_{1s}^{\text{SIDD}} = 541 \pm 89 \pm 22 \text{ eV}. \quad (2)$$

Keeping this in mind, we obtained the new parameters for the $\bar{K}N - \pi\Sigma$ potentials, used in [1] and described in more details in [4]. The new one- and two-pole potentials reproducing the experimental data (2) will be denoted by $V_{\bar{K}N-\pi\Sigma}^{1,\text{SIDD}}$ and $V_{\bar{K}N-\pi\Sigma}^{2,\text{SIDD}}$ respectively. In fact, the potentials reproducing the SIDDHARTA data reproduce the KEK data as well since the 1σ region of the most recent experiment lies almost entirely inside the 1σ KEK region.

The potential in momentum representation has the form

$$V_I^{\bar{\alpha}\bar{\beta}}(k^{\bar{\alpha}}, k'^{\bar{\beta}}) = \lambda_I^{\bar{\alpha}\bar{\beta}} g^{\bar{\alpha}}(k^{\bar{\alpha}}) g^{\bar{\beta}}(k'^{\bar{\beta}}), \quad (3)$$

where indices $\bar{\alpha}, \bar{\beta} = 1, 2$ denote $\bar{K}N$ or $\pi\Sigma$ channel respectively, I is a two-body isospin. We used Yamaguchi form-factors in both channels for the one-pole potential $V_{\bar{K}N-\pi\Sigma}^{1,\text{SIDD}}$ and in the $\bar{K}N$ channel for the two-pole potential $V_{\bar{K}N-\pi\Sigma}^{2,\text{SIDD}}$:

$$g^{\bar{\alpha}}(k^{\bar{\alpha}}) = \frac{1}{(k^{\bar{\alpha}})^2 + (\beta^{\bar{\alpha}})^2}, \quad (4)$$

Table 1: Parameters of the new one- and two-pole $\bar{K}N - \pi\Sigma$ potentials: range $\beta^{\bar{\alpha}}$ (fm^{-1}), strength $\lambda_I^{\bar{\alpha}\bar{\beta}}$ (fm^{-2}) parameters, and the additional unitless parameter s of the two-pole model.

	$V_{\bar{K}N-\pi\Sigma}^{1,\text{SIDD}}$	$V_{\bar{K}N-\pi\Sigma}^{2,\text{SIDD}}$
$\beta^{\bar{K}N}$	3.52	3.64
$\beta^{\pi\Sigma}$	1.48	1.05
$\lambda_0^{\bar{K}\bar{K}}$	-1.2777	-1.3753
$\lambda_0^{\bar{K}\pi}$	0.5431	0.5577
$\lambda_0^{\pi\pi}$	0.1541	0.0518
$\lambda_1^{\bar{K}\bar{K}}$	$0.4960 - i 0.1932$	$0.6178 - i 0.1965$
$\lambda_1^{\bar{K}\pi}$	1.7085	1.9151
$\lambda_1^{\pi\pi}$	1.9444	1.9904
s	0.0000	-0.7604

while in the $\pi\Sigma$ channel for the two-pole $V_{\bar{K}N-\pi\Sigma}^{2,\text{SIDD}}$ we used the following form-factor

$$g^{\bar{\alpha}}(k^{\bar{\alpha}}) = \frac{1}{(k^{\bar{\alpha}})^2 + (\beta^{\bar{\alpha}})^2} + \frac{s(\beta^{\bar{\alpha}})^2}{[(k^{\bar{\alpha}})^2 + (\beta^{\bar{\alpha}})^2]^2}. \quad (5)$$

Therefore, the two-pole potential contains additional to the strength $\lambda_I^{\bar{\alpha}\bar{\beta}}$ and range $\beta_I^{\bar{\alpha}}$ parameters unitless parameter s .

The parameters of the new $V_{\bar{K}N-\pi\Sigma}^{1,\text{SIDD}}$ and $V_{\bar{K}N-\pi\Sigma}^{2,\text{SIDD}}$ potentials, as before, were obtained by fitting to experimental data on low-energy K^-p scattering and kaonic hydrogen. They are shown in Table 1. Both potentials reproduce the medium values of the threshold branching ratios γ and $R_{\pi\Sigma}$, where

$$\gamma = \frac{\Gamma(K^-p \rightarrow \pi^+\Sigma^-)}{\Gamma(K^-p \rightarrow \pi^-\Sigma^+)} = 2.36 \pm 0.04, \quad (6)$$

is the measured value [9, 10] and

$$R_{\pi\Sigma} = \frac{\Gamma(K^-p \rightarrow \pi^+\Sigma^-) + \Gamma(K^-p \rightarrow \pi^-\Sigma^+)}{\Gamma(K^-p \rightarrow \pi^+\Sigma^-) + \Gamma(K^-p \rightarrow \pi^-\Sigma^+) + \Gamma(K^-p \rightarrow \pi^0\Sigma^0)} \quad (7)$$

is the ratio, constructed from the measured R_c and R_n [9, 10]:

$$R_c = \frac{\Gamma(K^-p \rightarrow \pi^+\Sigma^-, \pi^-\Sigma^+)}{\Gamma(K^-p \rightarrow \text{all inelastic channels})} = 0.664 \pm 0.011, \quad (8)$$

$$R_n = \frac{\Gamma(K^-p \rightarrow \pi^0\Lambda)}{\Gamma(K^-p \rightarrow \text{neutral states})} = 0.189 \pm 0.015. \quad (9)$$

An “experimental” value for the $R_{\pi\Sigma}$ is

$$R_{\pi\Sigma} = \frac{R_c}{1 - R_n(1 - R_c)} = 0.709 \pm 0.011. \quad (10)$$

The elastic and inelastic K^-p cross-sections $K^-p \rightarrow K^-p$, $K^-p \rightarrow \bar{K}^0n$, $K^-p \rightarrow \pi^+\Sigma^-$, $K^-p \rightarrow \pi^-\Sigma^+$, and $K^-p \rightarrow \pi^0\Sigma^0$ are reproduced by the new potentials with the same accuracy as in the previous article (see Fig.7 of [1]).

The remaining characteristics of the $V_{\bar{K}N-\pi\Sigma}^{1,\text{SIDD}}$ and $V_{\bar{K}N-\pi\Sigma}^{2,\text{SIDD}}$ potentials are shown in Table 2. In particular, the “strong” pole positions z_1 and z_2 (in MeV) are presented there together with the $1s$ level shifts $\Delta E_{1s}^{K^-p}$ and widths $\Gamma_{1s}^{K^-p}$ (eV) of kaonic hydrogen. The strong K^-p scattering lengths, obtained from the Lippmann-Schwinger coupled-channel equations and, therefore, exactly corresponding to the $\Delta E_{1s}^{K^-p}$ and $\Gamma_{1s}^{K^-p}$ values, are shown as well. The same characteristic of the $V_{\bar{K}N-\pi\Sigma}^{1,\text{KEK}}$ and $V_{\bar{K}N-\pi\Sigma}^{2,\text{KEK}}$ potentials, taken from Table II of [1], are also presented in the table. It is useful for investigation of the role of the poles of the $\Lambda(1405)$ resonance in the three-body results. It is seen from Table 2 that $V_{\bar{K}N-\pi\Sigma}^{1,\text{SIDD}}$ and $V_{\bar{K}N-\pi\Sigma}^{2,\text{SIDD}}$ potentials with different z_1 values and very close $\Delta E_{1s}^{K^-p}$, $\Gamma_{1s}^{K^-p}$ together with $V_{\bar{K}N-\pi\Sigma}^{1,\text{KEK}}$ and $V_{\bar{K}N-\pi\Sigma}^{2,\text{KEK}}$ with equal z_1 and different $\Delta E_{1s}^{K^-p}$, $\Gamma_{1s}^{K^-p}$ supplement each other.

The parameters of the highest strong pole z_1 for $V_{\bar{K}N-\pi\Sigma}^{1,\text{SIDD}}$ and $V_{\bar{K}N-\pi\Sigma}^{2,\text{SIDD}}$ differ significantly from the PDG values of the mass and width of the $\Lambda(1405)$ resonance [11]:

$$M_{\Lambda(1405)}^{PDG} = 1406.5 \pm 4.0 \text{ MeV}, \quad \Gamma_{\Lambda(1405)}^{PDG} = 50 \pm 2.0 \text{ MeV}. \quad (11)$$

However, the elastic $\pi^0\Sigma^0$ cross-sections obtained with the potentials have peaks with the maxima, which almost coincide with the $M_{\Lambda(1405)}^{PDG}$ value (for $V_{\bar{K}N-\pi\Sigma}^{2,\text{SIDD}}$) or is closer to it than $Re(z_1)$ ($V_{\bar{K}N-\pi\Sigma}^{1,\text{SIDD}}$), see Fig. 1. The widths of the peaks are within experimental errors of $\Gamma_{\Lambda(1405)}^{PDG}$.

In the three-body equations we used isospin-averaged masses for the particles instead of the physical ones. Inserted into the Lippmann-Schwinger equations with isospin-averaged masses the $\bar{K}N - \pi\Sigma$ potentials with parameters shown in Table 1 give K^-p scattering lengths $a_{K^-p}^{\text{aver}}$, which are different from the “physical” a_{K^-p} values. We show them in Table 2 together with $a_{\bar{K}N,0}^{\text{aver}}$ and $a_{\bar{K}N,1}^{\text{aver}}$, which are the $\bar{K}N$ scattering lengths for isospin $I = 0$ and $I = 1$ states respectively. In the case of the isospin-averaged masses $a_{\bar{K}N,1}^{\text{aver}}$ coincides with the K^-n scattering length.

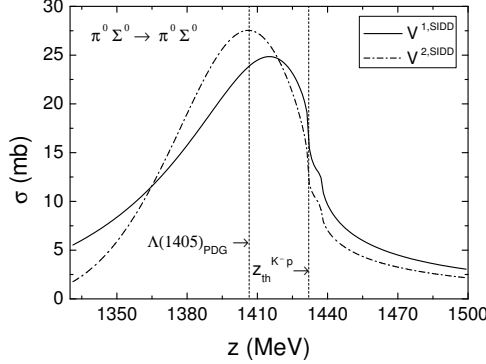


Figure 1: Elastic $\pi^0\Sigma^0$ cross-sections, obtained with $V_{\bar{K}N-\pi\Sigma}^{1,\text{SIDD}}$ (solid line) and $V_{\bar{K}N-\pi\Sigma}^{2,\text{SIDD}}$ (dash-dotted line) potentials. PDG value of the mass of $\Lambda(1405)$ resonance and K^-p threshold are shown as well (vertical lines).

The pole positions z_1 and z_2 remain almost unchanged, the K^-p “averaged” cross-sections do not manifest \bar{K}^0n threshold, but still describes the experimental data very well (see Fig. 7 of [1]).

2.2. Three-body formalism and the rest of the two-body input

The near-threshold elastic K^-d amplitudes were obtained using the Faddeev-type Alt-Grassberger-Sandhas (AGS) equations with coupled $\bar{K}NN$ and $\pi\Sigma N$ channels, described in details in [1]. The total energy of the K^-d system was considered up to the three-body $\bar{K}NN$ breakup threshold, where kinetic energy of the relative $K^- - d$ motion z_{kin} is equal to the deuteron binding energy E_{deu} .

The spin of the K^-d system is equal to one, the isospin to one half. All two-body potentials as well as the corresponding to them two-body T -matrices, being an input for the three-body calculations, were chosen to have zero orbital momentum. The total orbital momentum was also chosen equal to zero, therefore, the total angular momentum of the three-body system is equal to one. The calculations were performed in the momentum representation with proper antisymmetrization, necessary due to presence of the two baryons in every channel. The obtained system of ten integral equations was solved numerically, the logarithmic singularities in the $\pi\Sigma N$ channel and a pole at the deuteron binding energy were properly taken into account.

In contrast to the two-body coupled-channel equations for the $\bar{K}N - \pi\Sigma$ potentials construction, we neither included Coulomb interaction nor used physical masses for the particles in the three-body equations. The effect

of inclusion of the physical masses of K^- and \bar{K}^0 into AGS equation was studied recently in [12]. It makes 2% difference from the case of isospin-averaged masses for the real part of the K^-d scattering length, while the imaginary part remains almost unchanged.

We used one or two-term separable potentials, which are isospin and spin dependent. The new one- and two-pole $\bar{K}N - \pi\Sigma$ potentials reproducing the SIDDHARTA data on kaonic hydrogen are described in the previous subsection. In spite of the fact that SIDDHARTA experimental results (2) are more accurate than KEK data (1), we used the $V_{\bar{K}N-\pi\Sigma}^{1,\text{KEK}}$ and $V_{\bar{K}N-\pi\Sigma}^{2,\text{KEK}}$ potentials from Ref. [1] as well for investigation of the role of the poles of the $\Lambda(1405)$ resonance in the three-body results. As for the rest of the potentials necessary for the calculations, we used the best NN and ΣN potentials from the previous calculation and, as before, neglected πN interaction (due to its weakness in the $l = 0$ state).

The two-term NN potential $V_{NN}^{\text{TSA-B}}$ [13] (Eqs.(13) and (19) of [1]), chosen for the present calculation, accurately reproduces Argonne V18 phase shifts and, therefore, is repulsive at short distances. It gives correct scattering length $a = -5.413$ fm, effective range $r_{\text{eff}} = 1.760$ fm of the 3S_1 NN state and accurate binding energy of the deuteron $E_{\text{deu}} = 2.2246$ MeV. We used exact optical spin-dependent potential $V_{\Sigma N}^{\text{Sdep,Opt}}$ constructed in [1] for description of the $\Sigma N(-\Lambda N)$ interaction. The potential reproduces the experimental data on ΣN and ΛN scattering quite well.

2.3. Elastic K^-d amplitudes: results

The K^-d scattering lengths obtained using the new one- and two-pole $\bar{K}N - \pi\Sigma$ potentials, reproducing the SIDDHARTA data on kaonic hydrogen, are shown in Fig. 2 (black circle for $a_{K^-d}^{1,\text{SIDD}}$ and black square for $a_{K^-d}^{2,\text{SIDD}}$) together with our representative a_{K^-d} values from [1], obtained using the $V_{\bar{K}N-\pi\Sigma}^{1,\text{KEK}}$ and $V_{\bar{K}N-\pi\Sigma}^{2,\text{KEK}}$ potentials (half-empty circle and half-empty square respectively). They are also shown in Table 2, where we collect two-body and three-body characteristics of all four our $\bar{K}N - \pi\Sigma$ potentials.

It is seen, that the imaginary parts of the new $a_{K^-d}^{\text{SIDD}}$ are larger than those of the previous $a_{K^-d}^{\text{KEK}}$ by 20% for the one-pole and by 10% for the two-pole versions. The real parts are not so different, especially for the one-pole potentials. However, the main difference of the new results from those of [1] is that the K^-d scattering lengths obtained with the one- and two-pole

Table 2: Physical characteristics of the $V_{\bar{K}N-\pi\Sigma}^{1,SIDD}$ and $V_{\bar{K}N-\pi\Sigma}^{2,SIDD}$ potentials: strong pole positions z_1 and z_2 (MeV), K^-p scattering length a_{K^-p} (fm), kaonic hydrogen $1s$ level shift $\Delta E_{1s}^{K^-p}$ and width $\Gamma_{1s}^{K^-p}$ (eV). The same values for the $V_{\bar{K}N-\pi\Sigma}^{1,KEK}$ and $V_{\bar{K}N-\pi\Sigma}^{2,KEK}$ potentials are taken from [1]. Scattering lengths, calculated with isospin-averaged masses: $a_{K^-p}^{\text{aver}}$, $a_{\bar{K}N,0}^{\text{aver}}$ and $a_{\bar{K}N,1}^{\text{aver}}$ are also presented. The three-body characteristics, obtained using the corresponding $\bar{K}N - \pi\Sigma$ potentials, are shown as well: K^-d scattering length a_{K^-d} (fm) (a_{K^-d} values obtained using $V_{\bar{K}N-\pi\Sigma}^{1,KEK}$ and $V_{\bar{K}N-\pi\Sigma}^{2,KEK}$ potentials are taken from [1]), effective range $r_{K^-d}^{\text{eff}}$ (fm), and kaonic deuterium characteristics $\Delta E_{1s}^{K^-d}$ and width $\Gamma_{1s}^{K^-d}$ (eV).

	$V_{\bar{K}N-\pi\Sigma}^{1,SIDD}$	$V_{\bar{K}N-\pi\Sigma}^{2,SIDD}$	$V_{\bar{K}N-\pi\Sigma}^{1,KEK}$	$V_{\bar{K}N-\pi\Sigma}^{2,KEK}$
z_1	$1426 - i\,48$	$1414 - i\,58$	$1409 - i\,36$	$1409 - i\,36$
z_2	—	$1386 - i\,104$	—	$1381 - i\,105$
a_{K^-p}	$-0.76 + i\,0.89$	$-0.74 + i\,0.90$	$-1.00 + i\,0.68$	$-0.96 + i\,0.80$
$\Delta E_{1s}^{K^-p}$	-313	-308	-377	-373
$\Gamma_{1s}^{K^-p}$	597	602	434	514
$a_{K^-p}^{\text{aver}}$	$-0.52 + i\,0.81$	$-0.48 + i\,0.82$	$-0.80 + i\,0.62$	$-0.72 + i\,0.73$
$a_{\bar{K}N,0}^{\text{aver}}$	$-1.45 + i\,0.86$	$-1.45 + i\,0.86$	$-1.60 + i\,0.67$	$-1.62 + i\,0.78$
$a_{\bar{K}N,1}^{\text{aver}}$	$0.41 + i\,0.75$	$0.48 + i\,0.77$	$-0.004 + i\,0.56$	$0.18 + i\,0.67$
a_{K^-d}	$-1.48 + i\,1.22$	$-1.51 + i\,1.23$	$-1.49 + i\,0.98$	$-1.57 + i\,1.11$
$r_{K^-d}^{\text{eff}}$	$0.68 - i\,1.33$	$0.67 - i\,1.35$	$0.55 - i\,1.15$	$0.62 - i\,1.19$
$\Delta E_{1s}^{K^-d}$	-781	-794	-767	-809
$\Gamma_{1s}^{K^-d}$	1010	1012	810	902

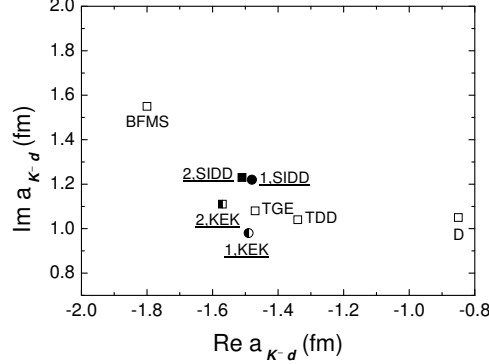


Figure 2: The results of the K^-d scattering length calculations using $V_{\bar{K}N-\pi\Sigma}^{1,\text{SIDD}}$ (black circle) and $V_{\bar{K}N-\pi\Sigma}^{2,\text{SIDD}}$ (black square) potentials. Results of our previous calculations [1] with one- (half-empty circle) and two-pole (half-empty square) representative potentials reproducing KEK data on kaonic hydrogen are shown as well together with earlier a_{K^-d} results: BFMS [14], TGE [15], TDD [16], D [17] (empty squares).

$\bar{K}N - \pi\Sigma$ potentials reproducing the SIDDHARTA data on kaonic hydrogen are very close one to the other, while our $a_{K^-d}^{\text{KEK}}$ values obtained with the one- and two-pole potentials are rather different. Therefore, it is not possible to resolve the question of the number of the poles forming the $\Lambda(1405)$ resonance from the results on near-threshold elastic K^-d scattering.

Four more values of the K^-d scattering length from Refs. [14, 15, 16, 17] (empty squares), where the Faddeev equations were also used, are shown in the Fig. 2 as well. Three of them [14, 15, 16] were obtained with coupled channels, while the fourth one [17] is a result of a single-channel calculation. The four a_{K^-d} values were compared with our previous results in [1], and since our present a_{K^-d} values are not too far from the previous ones, it is not necessary to repeat the discussion. We do not show results obtained using Fixed Scatterer Approximation since it was shown in [1], that the method is not a proper approach for the K^-d system.

The elastic amplitudes of K^-d scattering for kinetic energy from zero to E_{deu} calculated using four versions of $\bar{K}N - \pi\Sigma$ potentials are shown in Fig. 3. They are presented in a form of $k \cot \delta(k)$ function. Real (thick lines) and imaginary (thin lines) parts of the function obtained with $V_{\bar{K}N-\pi\Sigma}^{1,\text{SIDD}}$ (dashed lines), $V_{\bar{K}N-\pi\Sigma}^{2,\text{SIDD}}$ (solid lines), $V_{\bar{K}N-\pi\Sigma}^{1,\text{KEK}}$ (dotted lines) and $V_{\bar{K}N-\pi\Sigma}^{1,\text{KEK}}$ (dash-dotted lines) potentials are plotted. The chosen representation of the results demonstrates that the elastic near-threshold K^-d amplitudes can be approximated

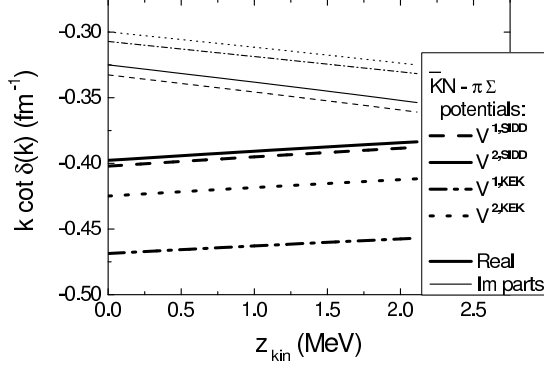


Figure 3: Real (thick lines) and imaginary (thin lines) parts of the elastic near-threshold K^-d amplitudes presented in a form of $k \cot \delta(k)$ function. The results obtained from the coupled-channel three-body AGS equations using $V_{\bar{K}N-\pi\Sigma}^{1,\text{SIDD}}$ (dashed lines), $V_{\bar{K}N-\pi\Sigma}^{2,\text{SIDD}}$ (solid lines), $V_{\bar{K}N-\pi\Sigma}^{1,\text{KEK}}$ (dotted lines) and $V_{\bar{K}N-\pi\Sigma}^{2,\text{KEK}}$ (dash-dotted lines) potentials are shown.

by the effective range expansion rather accurately since the lines are almost straight. The calculated effective ranges $r_{K^-d}^{\text{eff}}$ of K^-d scattering are shown in Table 2.

3. Kaonic deuterium

Mixture of the strong and Coulomb interaction makes investigation of low levels of hadronic atoms with the help of the Faddeev equations difficult. Due to this we constructed a complex two-body $K^- - d$ potential and used it for investigation of the $1s$ level of kaonic deuterium by Lippmann-Schwinger equation.

A one-term separable potential is too simple for reproducing the K^-d amplitudes obtained using AGS equations, therefore we chose the two-term form:

$$V_{K^-d}(\vec{k}, \vec{k}') = \lambda_{1,K^-d} g_1(\vec{k}) g_1(\vec{k}') + \lambda_{2,K^-d} g_2(\vec{k}) g_2(\vec{k}') \quad (12)$$

with Yamaguchi form-factors

$$g_i(k) = \frac{1}{\beta_{i,K^-d}^2 + k^2}, \quad i = 1, 2. \quad (13)$$

The complex strength parameters λ_{1,K^-d} and λ_{2,K^-d} were fixed by the conditions, that the V_{K^-d} potential reproduces the K^-d scattering length a_{K^-d} and the effective range $r_{K^-d}^{\text{eff}}$ obtained with one of the four $\bar{K}N - \pi\Sigma$

Table 3: Range $\beta_{i,K-d}$ (fm^{-1}) and strength $\lambda_{i,K-d}$ (fm^{-2}) parameters of the two-term $V_{K-d}^{1,\text{SIDD}}$ and $V_{K-d}^{2,\text{SIDD}}$ potentials ($i = 1, 2$).

	$V_{K-d}^{1,\text{SIDD}}$	$V_{K-d}^{2,\text{SIDD}}$
$\beta_{1,K-d}$	0.7	0.7
$\beta_{2,K-d}$	1.0	1.0
$\lambda_{1,K-d}$	$-0.0051 - i 0.0012$	$-0.0056 - i 0.0016$
$\lambda_{2,K-d}$	$0.0096 - i 0.0420$	$0.0109 - i 0.0420$

potentials and shown in Table 2. Variation of the real $\beta_{1,K-d}$ and $\beta_{2,K-d}$ parameters allowed us to reproduce the full near-threshold amplitudes more accurately. As a result, the near-threshold amplitudes obtained from the three-body calculations $f_{K-d}^{(3)}$, are reproduced by the two-body $K^- - d$ potentials through the interval $[0, E_{\text{deu}}]$ with such accuracy, that the two-body functions $k \cot \delta^{(2)}(k)$ are indistinguishable from the three-body $k \cot \delta^{(3)}(k)$ in Fig.3.

We denote $K^- - d$ potentials, which reproduce three-body amplitudes obtained using $V_{\bar{K}N-\pi\Sigma}^{1,\text{SIDD}}$ and $V_{\bar{K}N-\pi\Sigma}^{2,\text{SIDD}}$ potentials, as $V_{K-d}^{1,\text{SIDD}}$ and $V_{K-d}^{2,\text{SIDD}}$ respectively ($V_{K-d}^{1,\text{KEK}}$ and $V_{K-d}^{2,\text{KEK}}$ are defined analogically). The parameters of the potentials are shown in Table 3. As is seen, both $\beta_{1,K-d}$ and $\beta_{2,K-d}$ parameters for every potential turned up to be much smaller then the corresponding $\beta^{\bar{K}N}$ parameter, as it can be expected having in mind the size of the deuteron.

The constructed two-body complex potentials V_{K-d} were used for calculation of the 1s atomic level of kaonic deuterium, we are interested in. Calculation of the binding energy of a two-body system, described by the Hamiltonian with strong V^S and Coulomb V^{Coul} interactions

$$H = H^0 + V^S + V^{\text{Coul}} \quad (14)$$

was performed, for example, in [4], where the one-term V^S describing interaction of the coupled $\bar{K}N$ and $\pi\Sigma$ channels was considered. For the two-term one-channel separable potential $V^S = V_{K-d}$, defined by Eq.(12), the binding energy condition can be written explicitly:

$$\begin{aligned} & \left[\lambda_{1,K-d}^{-1} - \langle g_1 | G^{\text{Coul}}(E_{1s}^{S+\text{Coul}}) | g_1 \rangle \right] \left[\lambda_{2,K-d}^{-1} - \langle g_2 | G^{\text{Coul}}(E_{1s}^{S+\text{Coul}}) | g_2 \rangle \right] \\ & - \langle g_1 | G^{\text{Coul}}(E_{1s}^{S+\text{Coul}}) | g_2 \rangle \langle g_2 | G^{\text{Coul}}(E_{1s}^{S+\text{Coul}}) | g_1 \rangle = 0, \end{aligned} \quad (15)$$

where G^{Coul} is the Coulomb Green's function

$$G^{Coul}(z) = (z - H^0 - V^{Coul})^{-1}. \quad (16)$$

The expression for the matrix element of the G^{Coul} function with the Yamaguchi form-factors $|g\rangle$, entering Eq.(15), can be found in [18].

The real part of the binding energy of the $1s$ level of the kaonic deuterium, obtained from Eq. (15), defines the $1s$ level shift:

$$\Delta E_{1s} = E_{1s}^{Coul} - \text{Re} \left(E_{1s}^{S+Coul} \right), \quad (17)$$

where E_{1s}^{Coul} is the pure Coulomb energy. The doubled imaginary part of the binding energy E_{1s}^{S+Coul} defines the width of the ground state Γ_{1s} .

4. Results

The level shifts $\Delta E_{1s}^{K^-d}$ and widths $\Gamma_{1s}^{K^-d}$ of kaonic deuterium obtained with the two-body V_{K-d} potentials are shown in Fig. 4. The characteristics of the $1s$ level of kaonic deuterium calculated using the four versions of the $K^- - d$ potential, are plotted in: black circle ($V_{K-d}^{1,SIDD}$), black square ($V_{K-d}^{2,SIDD}$), black-and-white circle ($V_{K-d}^{1,KEK}$) black-and-white square ($V_{K-d}^{2,KEK}$). The results are also shown in Table 2.

The $1s$ level characteristics of kaonic deuterium corresponding to the $V_{\bar{K}N-\pi\Sigma}^{1,KEK}$ and $V_{\bar{K}N-\pi\Sigma}^{2,KEK}$ potentials with one- and two-pole structure of the $\Lambda(1405)$ resonance respectively, differ by 5% in the level shifts and by 10% in the widths. It could give possibility to draw conclusions about nature of the $\Lambda(1405)$ resonance from comparison with some (precise enough) experimental data. However, the results corresponding to the $V_{\bar{K}N-\pi\Sigma}^{1,SIDD}$ and $V_{\bar{K}N-\pi\Sigma}^{2,SIDD}$ potentials have almost the same widths and very close shifts. Therefore, an experiment on the kaonic deuterium characteristics as well as the K^-d scattering data cannot give an answer to the question on the number of the poles forming the $\Lambda(1405)$ resonance. Moreover, rather large widths, especially those obtained with the new $\bar{K}N - \pi\Sigma$ potentials, rise the question whether it will be possible to measure these characteristics accurately.

Figure 4 also contains the results obtained using an approximate relation. A ‘‘corrected Deser’’ formula (Eq. (19) of [19]), connecting a scattering length with characteristics of a hadronic atom and, according to the authors, containing isospin-breaking corrections in respect to the original Deser formula [20], is widely used nowadays. It was shown in [4, 21], that the accuracy

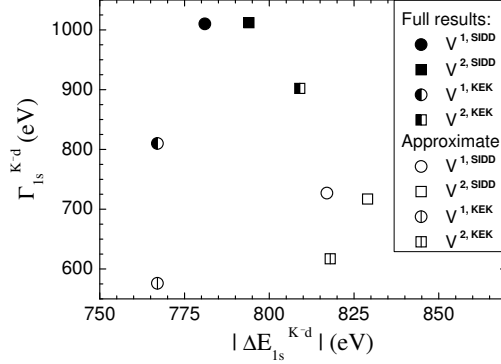


Figure 4: Level shifts and widths of kaonic deuterium, calculated with $V^{1,SIDD}$ (black circle), $V^{2,SIDD}$ (black square), $V^{1,KEK}$ (black-and-white circle) and $V^{2,KEK}$ (black-and-white square) potentials. Approximate values obtained using corrected Deser formula are also shown (white circle, white square, crossed circle and crossed square, respectively).

of the formula is about 10% for the two-body K^-p system. Obviously, the accuracy of the approximate formula should be less for the three-body K^-d system since three-body effects cannot be taken into account in it.

The $1s$ level shifts and widths of kaonic deuterium obtained from the corrected Deser formula using four our a_{K-d} values are shown in Fig. 4 in the empty circle ($a_{K-d}^{1,SIDD}$ is used), empty square ($a_{K-d}^{2,SIDD}$), vertically crossed circle ($a_{K-d}^{1,KEK}$) and vertically crossed square ($a_{K-d}^{2,KEK}$). The top index of a_{K-d} denotes the $\bar{K}N - \pi\Sigma$ potential, which was used in the AGS equations. It is seen, that the level shifts obtained using the approximate formula are very close to ours for the KEK and have 4% difference for the SIDDHARTA K^-d scattering lengths. As for the width of the $1s$ atom level, the approximate formula underestimates it at about 30% in comparison with all four our results, calculated using the two-body V_{K-d} potentials.

Now, in contrast to the kaonic hydrogen case, our results of the characteristics of kaonic deuterium cannot be called “exact”. However, the only shortcoming of our approach, which is the supposed structurelessness of the deuteron, is contained in the corrected Deser formula as well. Indeed, the only change, which can be made in the original formula for the K^-p system for it’s usage in the K^-d case, is the change of the corresponding reduced mass. Thus, the deuteron structure is not taken into account in the approximate formula. In contrast to [19], we made no additional approximations, therefore, our approach is much more accurate.

Table 2 containing several two-body characteristics of the four $\bar{K}N - \pi\Sigma$ potentials and the corresponding to them three-body K^-d scattering and kaonic deuterium observables allows us to reveal the role of the $\bar{K}N - \pi\Sigma$ interaction. Indeed, the three-body formalisms together with the two-body input, except the main interaction, are the same in all three-body calculations. Therefore, differences between a_{K^-d} , $r_{K^-d}^{\text{eff}}$, $\Delta E_{1s}^{K^-d}$ and $\Gamma_{1s}^{K^-d}$ are caused by differences of the $V_{\bar{K}N-\pi\Sigma}^{1,\text{KEK}}$, $V_{\bar{K}N-\pi\Sigma}^{2,\text{KEK}}$, $V_{\bar{K}N-\pi\Sigma}^{1,\text{SIDD}}$ and $V_{\bar{K}N-\pi\Sigma}^{2,\text{SIDD}}$ potentials.

Data in Table 2 confirms, that the K^-d scattering lengths have no correlation with z_1 (and z_2) pole properties at all: equal z_1 values for the two potentials reproducing the KEK data lead to sufficiently different $a_{K^-d}^{1,\text{KEK}}$ and $a_{K^-d}^{2,\text{KEK}}$ values. And conversely, very close K^-d scattering lengths were obtained with $V_{\bar{K}N-\pi\Sigma}^{1,\text{SIDD}}$ and $V_{\bar{K}N-\pi\Sigma}^{2,\text{SIDD}}$, which are characterised by rather different z_1 values. The same is true for the effective range $r_{K^-d}^{\text{eff}}$, level shift $\Delta E_{1s}^{K^-d}$ and width $\Gamma_{1s}^{K^-d}$ of kaonic deuterium. Therefore, there is no correlation between the pole or poles of the $\Lambda(1405)$ resonance described by a $\bar{K}N - \pi\Sigma$ potential and the three-body K^-d elastic scattering or kaonic deuterium characteristic obtained using the potentials.

On the other hand, there is a clear correlation between the imaginary parts of the K^-d scattering length a_{K^-d} and the width of kaonic deuterium $\Gamma_{1s}^{K^-d}$ – the same as between the two-body $\text{Im } a_{K^-p}$ and $\Gamma_{1s}^{K^-p}$. Such property was used in the original Deser formula [20] already, but the dependence definitely differs from the original Deser as well as the corrected Deser functional form for the K^-p and K^-d systems.

5. Conclusions

We calculated $1s$ level shift $\Delta E_{1s}^{K^-d}$ and width $\Gamma_{1s}^{K^-d}$ of kaonic deuterium, corresponding to the new $\bar{K}N - \pi\Sigma$ potentials, reproducing SIDDHARTA data on kaonic hydrogen. Our previous potentials, reproducing KEK data, were used as well. The results were obtained from the Lippmann-Schwinger equation with directly included Coulomb and the strong two-body $K^- - d$ potential. The $K^- - d$ potentials reproduce the three-body characteristics: a_{K^-d} , $r_{K^-d}^{\text{eff}}$ and the elastic near-threshold K^-d amplitudes, which were calculated using the coupled-channel AGS equations. All results are shown in Table 2 together with several characteristics of the four $\bar{K}N - \pi\Sigma$ potentials.

We also checked, whether it is possible to resolve the question of the number of poles forming $\Lambda(1405)$ resonance from comparison of theoretical

predictions with eventual experimental data on low-energy K^-d scattering or kaonic deuterium. For this purpose the one- and two-pole versions of the $\bar{K}N - \pi\Sigma$ potentials were used. We found, that the question cannot be resolved in such a way since the results, corresponding to the new one- and two-pole $\bar{K}N - \pi\Sigma$ potentials are very close. Moreover, it is seen from Table 2 that there is no correlation between the pole or poles of the $\Lambda(1405)$ resonance described by a $\bar{K}N - \pi\Sigma$ potential and the three-body K^-d elastic scattering or kaonic deuterium characteristic obtained using the potential.

The calculated widths of the $1s$ level of kaonic deuterium are rather large, thus the question of possibility of accurate measuring the atomic characteristics rises. We demonstrated, that the corrected Deser formula, widely used for estimation of the $1s$ level shift and width of kaonic atoms, considerably underestimates the width of kaonic deuterium.

Acknowledgments

The author is thankful to J. Révai for fruitful discussions. The work was supported by the GACR grant P202/12/2126.

References

- [1] N.V. Shevchenko, Phys. Rev. C 85, 034001 (2012).
- [2] Mini-Proceedings ECT* Workshop "Hadronic Atoms and Kaonic Nuclei", (ECT*, Trento, Italy, October 12–16, 2009), Eds. C. Curceanu and J. Marton; nucl-ex/1003.2328.
- [3] Mini-Proceedings ECT* Workshop "Strangeness in Nuclei", (ECT*, Trento, Italy, October 04–08, 2010), Eds. C. Curceanu and J. Zmeskal; nucl-ex/1104.1926.
- [4] J. Révai, N.V. Shevchenko, Phys. Rev. C 79, 035202 (2009).
- [5] C. Curceanu (Petrascu) *et al.*, Few-Body Syst. 50, 447 (2011).
- [6] M. Bazzi *et al.*, Phys. Lett. B 704, 133 (2011).
- [7] R.C. Barrett, A. Deloff, Phys. Rev. C 60, 025201 (1999).
- [8] M. Iwasaki *et al.*, Phys. Rev. Lett. 78, 3067 (1997); T.M. Ito *et al.*, Phys. Rev. C 58, 2366 (1998).

- [9] D.N. Tovee *et al.*, Nucl. Phys. B 33, 493 (1971).
- [10] R.J. Nowak *et al.*, Nucl. Phys. B 139, 61 (1978).
- [11] K. Nakamura *et al.* (Particle Data Group), J. Phys. G 37, 075021 (2010).
- [12] J. Révai, nucl-th/1203.1813.
- [13] P. Doleschall, *private communication*.
- [14] A. Bahaoui, C. Fayard, T. Mizutani, B. Saghai, Phys. Rev. C 68, 064001 (2003).
- [15] G. Toker, A. Gal, J.M. Eisenberg, Nucl. Phys. A 362, 405 (1981).
- [16] M. Torres, R.H. Dalitz, A. Deloff, Phys. Lett. B 174, 213 (1986).
- [17] A. Deloff, Phys. Rev. C 61, 024004 (2000).
- [18] W. Schweiger *et al.*, Phys. Rev. C 27, 515 (1983).
- [19] U.-G. Meißner, U. Raha, A. Rusetsky, Eur. Phys. J. C 35, 349 (2004).
- [20] S. Deser *et al.*, Phys. Rev. 96, 774 (1954).
- [21] A. Cieplý, J. Smejkal, Eur. Phys. J. A 34, 237 (2007) .